Final Report:

Use of ROV Video for Rapid Estimates of Discharge Rates from Submerged Oil Leaks

by

Frank Shaffer, USDOE National Energy Technology Laboratory

Ömer Savaş, U.C. Berkeley, Department of Mechanical Engineering

funded by

United States Department of Energy, National Energy Technology Laboratory

and

United States Department of Interior, Bureau of Safety and Environmental Enforcement
BSEE Project E13PG00053, BSEE-NETL WFO Project 2810143

Contents

ABSTRACT

This report describes how to use video of a submerged oil leak jet to quickly estimate the discharge rate. Video is usually available from Remotely Operated Vehicles (ROV). This approach was first developed by the Flow Rate Technical Group (FRTG) Plume Analysis Team to estimate the discharge rate from the Deepwater Horizon oil leak. The authors were members of the FRTG Plume Analysis Team.

The approach uses ROV video to measure the velocity of visible features that propagate along the boundary of an opaque oil leak jet. The visible features include turbulent eddies, vortices, and particles entrained in the jet fluid. The velocity of visible features at the jet boundary can be used to estimate the internal velocity profiles of the leak jet. Once the internal velocity profiles are estimated, the jet discharge rate can be calculated.

Two approaches are described to measure the velocity of visible features: a manual tracking approach and an approach using automated software. The manual approach can be applied quickly (an hour or less) and can use video from ROV cameras at standard frame rates (in the range of 30 to 60 frames per second). The automated approach can also be applied quickly (hours), but may require higher frame rates.

BACKGROUND

During the Deepwater Horizon (DWH) oil leak, in May of 2010, the Flow Rate Technical Group (FRTG) was charged with generating official government estimates of the oil leak rate [McNutt et al.]. The Plume Team of the FRTG was given ROV video of the oil leak jets and asked to quickly produce the first official estimates of the leak rate. The basic approach developed by the Plume Team was to measure the velocity of visible features (turbulent eddies, vortices, entrained particles of hydrates and waxes) at the boundary of the opaque oil jets. The boundary velocity was then used to estimate the internal velocity profiles of the oil jets.

Figure 1 shows large visible features propagating at the boundary of the DWH oil leak jet through consecutive video frames from an ROV camera. Due to the low frame rate of PAL cameras (25 per second) used on ROVs for the DWH, only large features persist over the time between camera frames. Smaller features deform quickly and may not persist over the frame interval time. Features that persist from camera frame to camera frame, are referred to as "coherent" features.

Boundary velocities can be used to estimate internal velocity profiles. With the internal velocity profiles -- and with assumptions for the amount of entrained water, amount of gas dissolved in the oil, and the jet diameter -- an estimate of the total discharge rate can be calculated (as explained below). Before continuing the discussion of this approach, a brief discussion of the theory of turbulent jets is helpful.

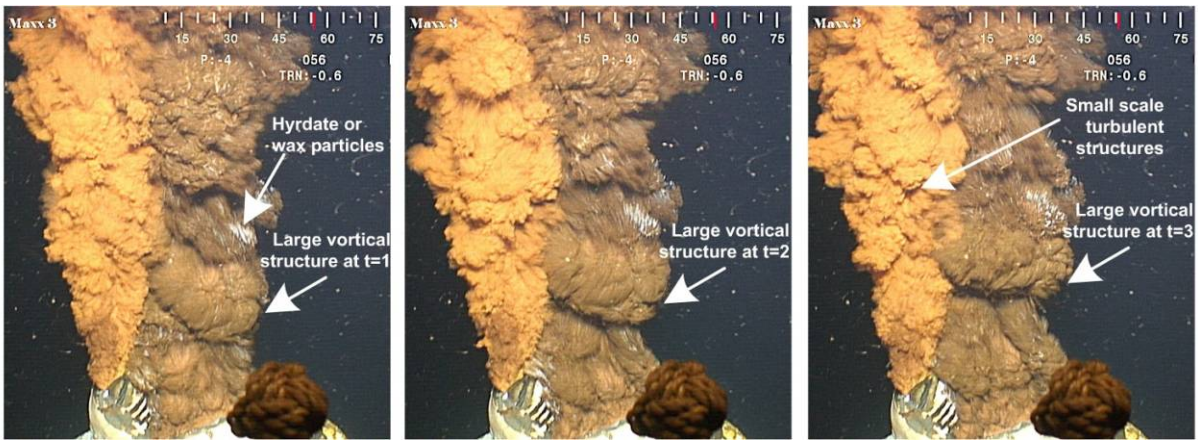

Figure 1. Consecutive video frames showing examples of visible features propagating in the flow direction on the Deepwater Horizon oil leak jet. The jet diameter was approximately 50 cm and the video frame rate was 25 per second.

Theory of Submerged Turbulent Jets

The theory of submerged turbulent jets is well established. Prandtl (1925) and others developed the theoretical foundation in the 1910's and 1920's. Abramovich (1963), Schlichting (2004) and others made advances in both experiments and theory from the 1930's through the 1950's. With recent advances in computational fluid dynamics (CFD), the time-averaged behavior of submerged turbulent jets can be accurately simulated (Eggers, 2007; Guo, 2000; Trujillo, 2007).

Figure 2 illustrates the velocity profiles of a fully developed turbulent pipe flow emitting into an infinite body of fluid at rest. Because the mean streamwise velocity (velocity in the direction of the jet) of a submerged turbulent jet is orders of magnitude higher than the mean radial velocity

(velocity normal to the direction of the jet), the radial velocity can be ignored in many practical applications and will be ignored in this application. For the remainder of this report, “velocity” will be defined as streamwise velocity in the x-direction of the jet centerline.

When a submerged turbulent jet discharges into an infinite body of fluid at rest, the edges of the jet shear against the surrounding fluid causing the formation of a "mixing layer." The mixing layer causes entrainment of the surrounding fluid into the jet, thereby causing the jet diameter to expand. As illustrated in Figure 2, the radial profile of velocity begins as nearly flat at the jet exit, then the shearing action causes the radial profile of velocity to transform into a Gaussian profile. All submerged turbulent jets have a divergence angle around 24 degrees (half angle of 12 degrees) [Lee, 2003; Albertson, 1950; Miller & Comings, 1957; and Bradbury, 1965]. The "statistical jet boundary" lines converge at a focal point at a distance of $2.5D_{jet}$ upstream of the jet exit, which is referred to as the virtual origin.

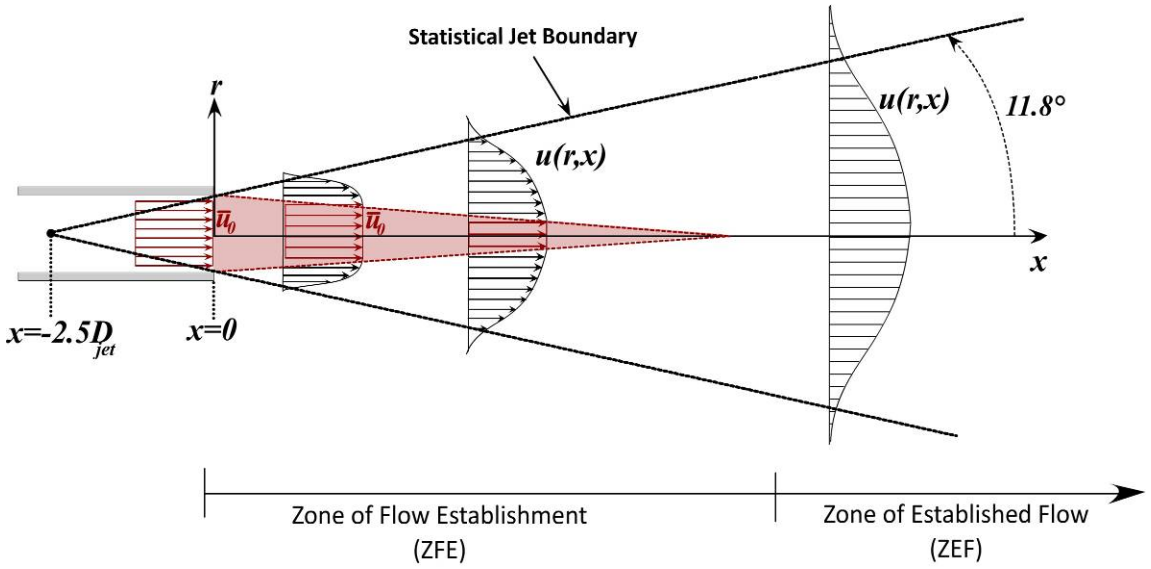

Figure 2. Velocity profiles and regions of a submerged turbulent jet.

The distance from the jet exit to the point where velocity drops below the mean exit velocity, $\overline{u}_0$ is called the Zone of Flow Establishment (ZFE). The ZFE has a constant velocity core, which in Figure 2 is shown as the red shaded area. For a submerged jet exiting from a fully developed pipe flow, the ZFE about six exit diameters long (Lee & Chu, 2003). The boundaries of the constant velocity core are formed by points where the velocity decreases infinitesimally below $\overline{u}_0$.

Downstream of the ZFE is the Established Flow Zone (EFZ). In the EFZ, radial profiles of mean streamwise velocity are Gaussian and self-similar. Self-similar means that at any distance, *x*, all data for mean velocity fall onto the same radial profile when plotted in the non-dimensional form of $u(r)/u_c$ and r/R_{jet}, where u_c is the centerline velocity at *x,* and R_{jet} is the radius of the jet at *x*.

Lee and Chu (2003) derive equations for the radial profiles of velocity and concentration in a submerged turbulent jet. In the ZFE, inside the constant velocity core, for $r < R_{core}(x)$, where $R_{core}(x)$

is the half width of the constant velocity core, the velocity and concentration (fraction of fluid at any point that is jet fluid) are given by

$$u(x,r)=u_0 \qquad c(x,r)=c_0 \tag{1}$$

In the ZFE, outside of the constant velocity core, where r > R_{core}, the velocity and concentration are given by

$$u=u_0\exp\left[-\frac{(r-R_{core}(x))^2}{b(x)^2}\right] \qquad c=c_0\exp\left[-\frac{(r-R_{core}(x))^2}{\lambda^2 b(x)^2}\right] \tag{2}$$

where *b* is the half width of the jet from the centerline to the statistical jet boundary, and λ is a turbulent diffusion coefficient. In the EFZ, the velocity profile is given by:

$$u=u(x,0)\exp\left[-\frac{r^2}{b(x)^2}\right] \qquad c=c(x,0)\exp\left[-\frac{r^2}{\lambda^2 b(x)^2}\right] \tag{3}$$

The half width of the jet is given by $b=\beta x$, where β is the slope of the statistical jet boundary. The experimental work of Albertson (1950) and Wygnanski and Fiedler (1969) found that $\beta=0.114$ for a submerged turbulent jet emitting from a round orifice. The diffusion coefficient, λ, is equal to the ratio of the divergence angle of the statistical concentration boundary to the divergence angle of the statistical jet boundary. Experimental work of Papanicolaou and List (1988) found that $\lambda=1.2$ for a submerged turbulent jet, indicating that the concentration half width is larger than the velocity half width.

Calculation of the Discharge Rate from a Submerged Turbulent Jet.

The following expression can be used to calculate discharge rates:

$$\dot{Q}_{oil}=\bar{u}(x)A_{jet}(x)[1-X_{GOR}]E(x) \tag{4}$$

where

$\bar{u}(x)$ is the average jet velocity at a distance, x, from the jet exit

$A_{jet}(x)$ is the cross sectional area of the jet at a distance, x, from the jet exit

X_{GOR} is the volume fraction of methane gas dissolved in the oil. The DWH leaks had significant amounts of supercritical methane in the oil.

$E(x)$ is the ratio of the volume of oil to the total jet volume (oil plus entrained surrounding fluid)

The jet cross sectional area, $A_{jet}(x)$, can be found from the ROV video.

The gas-to-oil ratio, X_{GOR}, can be estimated, or measured by sampling the jet fluid with ROV probes and bringing it to the surface for analysis (Schlumberger, 2010).

The entrainment parameter, $E(x)$, can be found by measuring the expansion of the jet, or by using theory such as that of Lee & Chu (2003) as described above in Equations 1-3.

The main challenge is to determine the relationship between the velocity of visible features, u_{vf}, and the mean velocity of the jet, $\bar{u}(x)$. The Plume Team overcame this challenge by making measurements of the velocity of visible features close to the jet exit, within, x/D <2, in the ZFE. An assumption was made that coherent structures this close to the jet exit are sampling the constant velocity core (moving at the velocity of the core). Entrainment was assumed to be negligible at x/D<2.

Manual Measurement of the Velocity of Visible Features

Manual feature tracking is simply using a mouse cursor (or other pointing device) to track visible, features from frame-to-frame through an ROV video. Figure 3 shows an example of manual tracking a large vortical feature through three consecutive video frames of the DWH post riser cut leak. The results are shown in the table below.

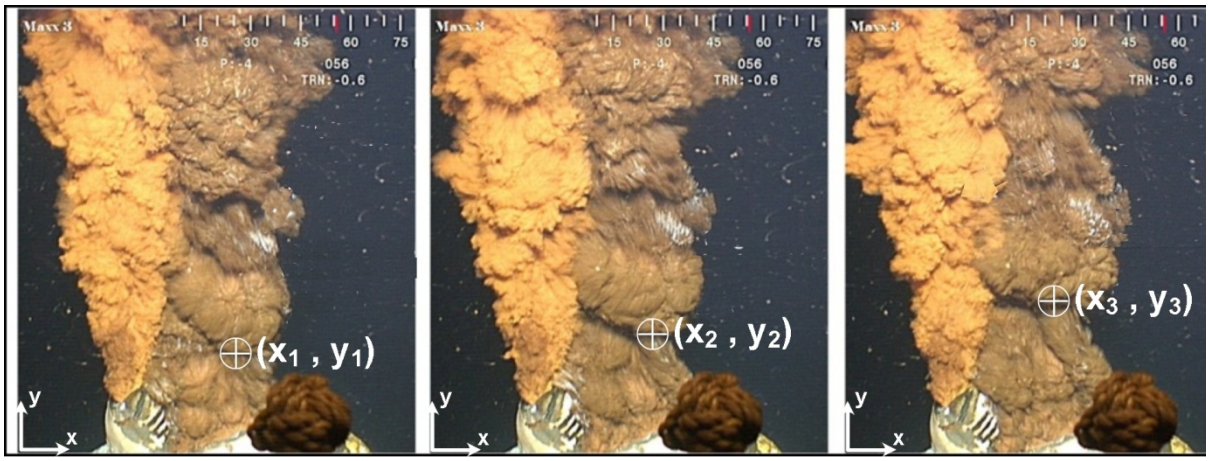

Figure 3. Manual tracking of a large eddy in the DWH post-riser cut jet.

Frame	x	y	DX	DY	DS
1	340	152			
2	350	197	10	45	46
3	360	245	10	48	49

Table 1. Positions of large visible feature through three video frames. Units in pixels.

The distances are in reference to an origin at the lower left corner of the video. The scale of the video is taken from measurement of a known distance; in this case, the diameter of the riser exit, 0.51 m. The scale is 1.91 mm/pixel. The frame rate of the PAL video camerasu used on DWH ROV's is 25 frames/sec, or 0.04 seconds between frames. The velocity from frame 1 to frame 2, and from frame 2 to 3, is found to be 2.3 m/s.

In this case, the MTrackJ plugin [Meijering] for the ImageJ image analysis suite from the National Institutes of Health (NIH) [Schneider] is used to track visible features. Both have advanced image analysis and tracking tools, and are available for free.

Manual Tracking Examples: The Deepwater Horizon Oil Leak Jets

There were three types of leaks from the DWH Macando Well: Riser Kink Jets, Riser End Jet, and Post Riser-cut Jet. The sections below are examples of manual tracking of these jets by Shaffer et al [FRTG].

Riser Kink Jet

The Riser Kink had several leak jets, but only one had a clear, unobstructed view. Figure 4 shows manual feature tracking for this jet. An average velocity of 1.7 m/s was measured at a distance of 0.6 meters downstream from the jet exit.

Figure 4: Manual feature tracing in the main jet of the Riser Kink Jets. (Trajectories were pseudocolored randomly to make them easier to see. The colors do not represent velocity magnitude).

Velocities measured for Riser End Jet

For the Riser End Jet, velocities were measured at two locations along the bottom edge of the jet (Figures 5). One location was 0.8 meters downstream from the jet exit and the other location was further downstream at 1.5 meters from the jet exit. Jet velocity was measured only when the jet was dark in color and assumed to be all oil[1].

[1] Oil and gas separated in the long distance to the riser end jet, producing an alternating slug flow of oil and gas.

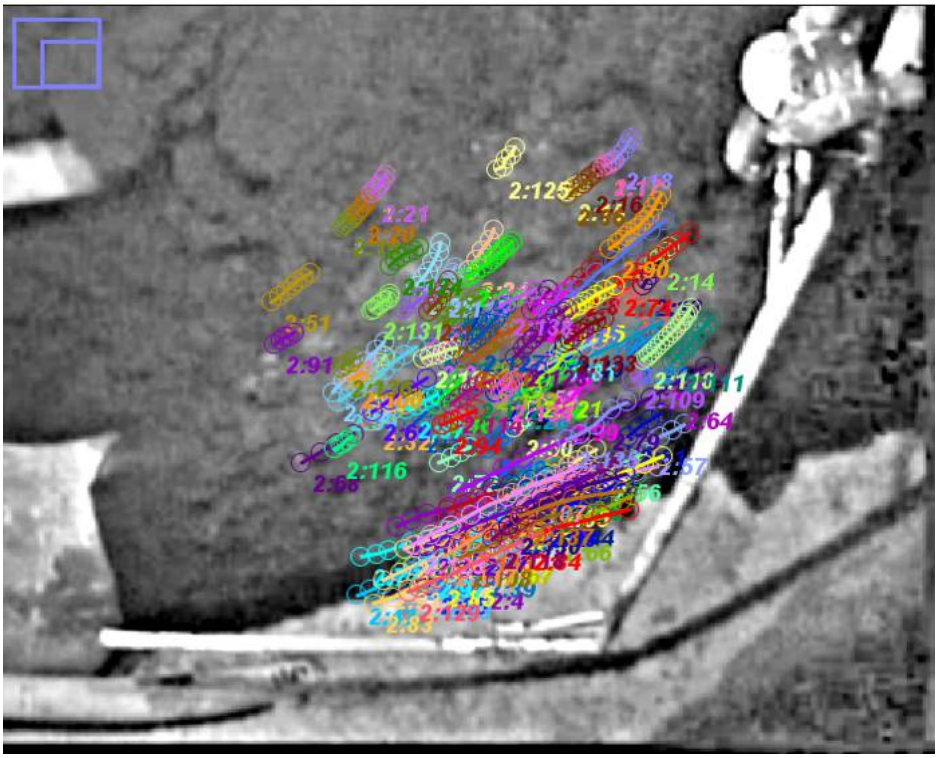

Figure 5: Manual feature tracking in the Riser End Jet.

Velocities measured in Post Riser-Cut Jet

For the Post Riser-Cut Jet, the features were tracked on frames 2810 to 3125 of the video "TOPHAT_06-03-10_14-29-22.avi." More than 500 features were tracked. The average distance downstream of the riser was 0.6 meters (about 1 jet diameter downstream). The average velocity measured was 1.5 meters per second. The plot below shows a histogram of the velocity measurements.

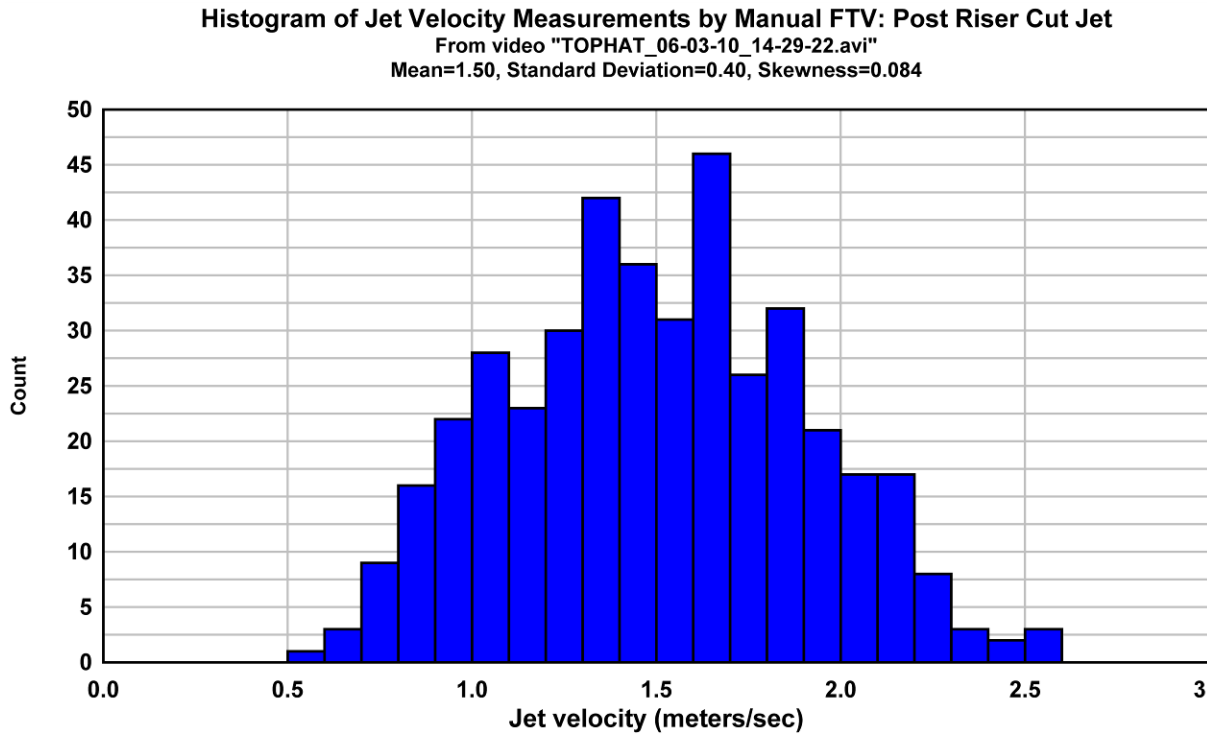

Figure 6. Histogram of velocity measurements by manual tracking in the post riser-cut jet. Mean velocity = 1.50 m/s; standard deviation = 0.40 m/s; skewness = 0.084 m/s.

Calculation of Discharge Rate for the Post Riser-Cut Jet:

The average discharge rate, $\dot{Q}_{oil}$, was calculated using Equation 4

$$\dot{Q}_{oil} = \bar{u}(x) A_{jet}(x)\left[1 - X_{GOR}\right] E(x)$$

The average velocity of visible features that propagated from frame-to-frame in the Post Riser-Cut Jet, $\bar{u}(x)$, was 1.5 m/s at an average location of 1.0 meters downstream of the jet exit. The average diameter of the jet at this location, $A_{jet}(x)$, was measured from ROV video to be 0.49 m, giving a cross sectional area of 0.19 m^2. The fluid mixture flowing out of the Post Riser Cut Jet is assumed to be a homogeneous mixture of oil and supercritical methane. The volume fraction of oil in this mixture was measured to be 0.29 at the sea floor and 0.4 at the sea surface [FRTG]. The discharge rate is measured in units of barrels of oil at the sea surface. The equation for oil discharge rate becomes

$$\dot{Q}_{oil} = 1.5 * 0.19 * 0.4 = 0.083 \, {}^{m^3}\!/_{s}$$

To convert this volumetric flow rate to barrels per day at the sea surface, conversion factors of 264.2 US liquid gallons per m^3/s and 42 US liquid gallons per barrel of crude oil are applied. Therefore, the total average oil leak rate from Post Riser-Cut Jet is calculated to be 61,000 barrels per day.

Automated Measurement of the Velocity of Visible Features

A type of object tracking called Image Correlation Velocimetry (ICV) can also be used to automatically measure the velocity of visible features. The use of automated software allows large amounts of video -- far too much for manual tracking -- to be analyzed quickly. A subcategory of ICV is called Particle Image Velocimetry (PIV) can be used for tracking visible features of turbulent jets [Shaffer et al.]. Traditionally, PIV is used to measure velocity fields in a transparent gas or liquid by seeding the flow with small (low Stokes number) particles that follow the fluid flow. Two consecutive video frames are selected and the second frame is divided into interrogation regions as shown in Figure 7. A smaller "template" region from the first frame is cross-correlated over the interrogation region of the second frame. The template cross-correlation can be described as

$$\Phi_{fg}(m,n) = \sum_{m}\sum_{n} f_1(i+m, j+n) g_2(i, j)$$

where $f_1(i, j)$ is the grey level array of template region in frame 1 and $g_2(i, j)$ is the grey level array of the interrogation region in frame 2. The subscripts m and n are the center position of the template over the interrogation region when a cross-correlation is calculated. The result is a correlation peak that measures the average displacement of the template region from frame 1 to frame 2. The correlation peak measures the average distance a visible feature moved from the first video frame to the second. With the time between video frames, Δt, a velocity vector can be calculated for each interrogation region. A threshold for the correlation peak can be set to reject poor correlations.

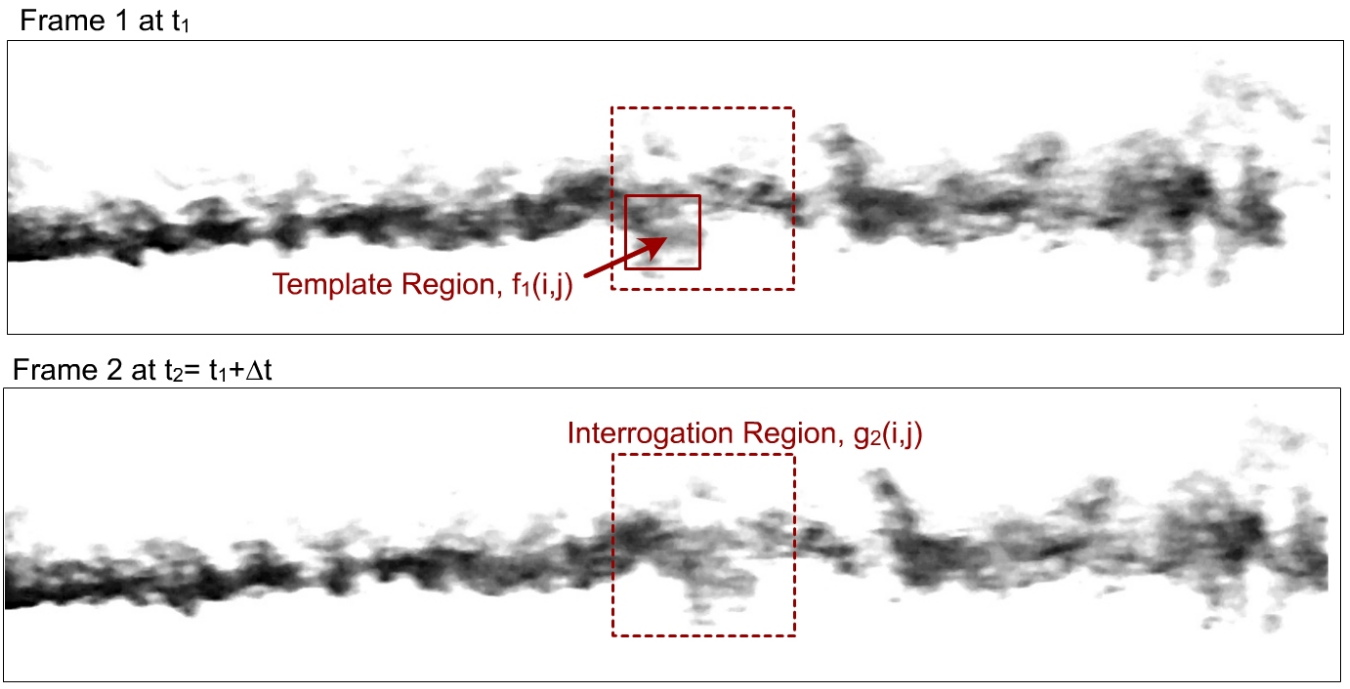

Figure 7. Illustration of template and interrogation regions in two consecutive video frames of dye colored features in water jet experiments at the UC Berkeley Tow Tank.

Verification of Automated PIV Measurement with UC Berkeley Water Tunnel Tests

To test and verify automated PIV software for tracking visible features of a submerged jet, experiments were conducted in the U.C. Berkeley Tow Tank. A dye colored water jet was used to simulate the visible features of the DWH jets. The flow circuit is shown in Figure 8. Jet exit diameters were 10.2 cm and 20.3 cm with flow rates up to 11 gallons/sec, producing Reynolds numbers in the range of the DWH oil leak jets (up to 500,000). The dye-colored water jets were recorded with high speed video and radial profiles of velocity were mapped with Laser Doppler Anemometry (LDA). Particle Image Velocimetry (PIV) software was applied to measure the velocity of visible features. The experiments and results are summarized below. For a thorough discussion see [Shaffer et al]. The velocities measured with PIV software were in good agreement with the LDA measurements.

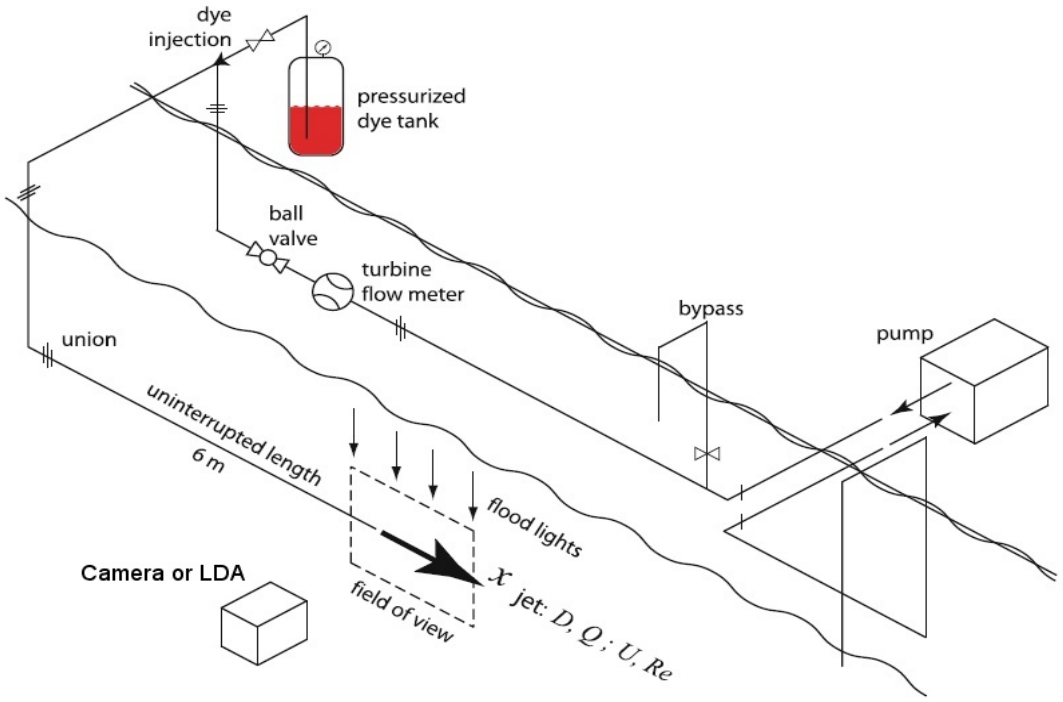

The dye-colored jets were recorded with a high definition, high speed video camera (Vision Research Model v341) at frame rates up to 1500 per second at resolutions up to 2560x1100 pixels. Two types of dye coloring of the water jet were used. The entire jet was dyed or “point” injection of dye was used.

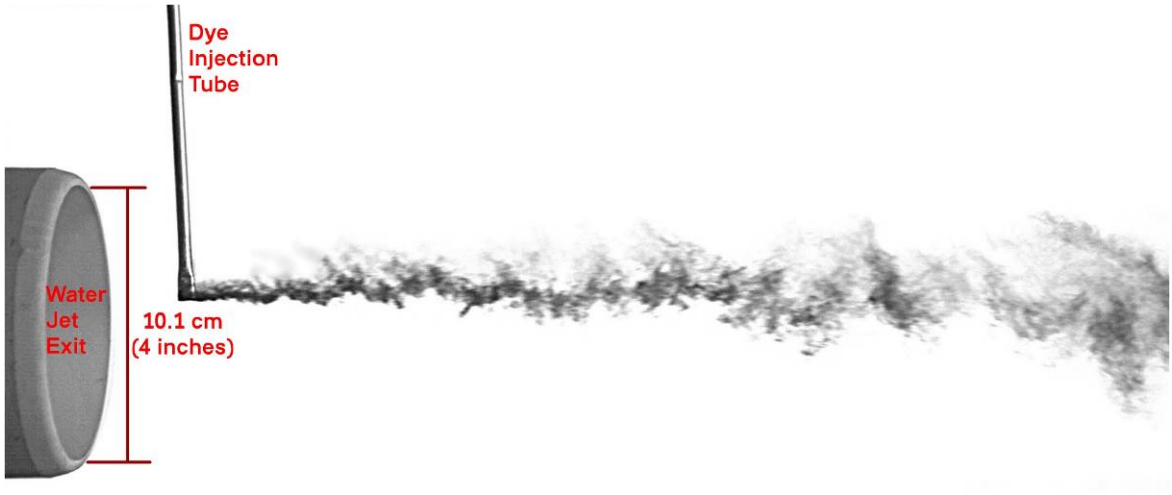

Figure 8. Flow visualization with dye point injection. Water flow rate was 41.7 liters/sec (11 gallons/sec) producing a Reynolds number of 500,000. The camera frame rate was 1500/second and the exposure time was 0.75 ms.

To measure the velocity of dyed flow features, the high speed video was analyzed with a PIV code developed by Q. Tseng (Tseng, 2011; Tseng, 2013). The code is implemented as a plugin for ImageJ, an image analysis tool developed by the National Institutes of Health (NIH) (Schneider, 2012). The PIV tool by Tseng is based on a template matching approach.

The radial profiles of streamwise velocity of the jet were also mapped with a Dantec FlowExplorer Laser Doppler Anemometer (LDA) (Dantec, 2013) at downstream distances of x/D_{jet} = 0.25, 2.0 and 4.0. A 300 mm focal length lens was used. The LDA was operated in non-coincidence mode. The jet flow was seeded with 50 micron diameter silver coated ceramic spheres of density 0.8-1.2 g/cm^3.

Laser Doppler Anemometry

Since submerged turbulent jets are self-similar, when normalized velocity is plotted against normalized radius, all data fall onto the same profile. Figure 9 shows normalized LDA data for a 10.2 cm diameter pipe jet measured at a distance of two jet diameters downstream of the exit.

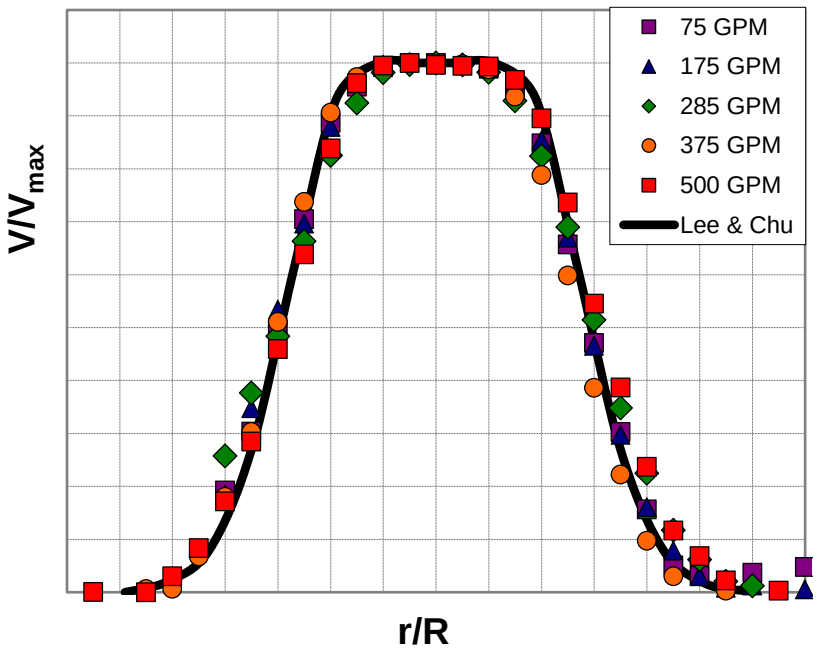

Figure 9. Normalized LDA data for a submerged water jet exiting from a 10.2 cm diameter pipe at various jet discharge rates. From the UC Berkeley Tow Tank.

Image Correlation Velocimetry of Dyed Flow Features

For the flow condition of 660 gallons/minute, a total of 44,867 video frames were recorded at 1150 frames/sec for a total sample period of 39.0 seconds. ICV was applied with as interrogation window of 200x200 pixels and a subregion template of 125 x 125 pixels. The center of the interrogation region was moved in steps of 50 pixels. The mean velocity at the jet centerline was 4.31 m/s. Figures 10 and 11 show good agreement between LDA and PIV measurements.

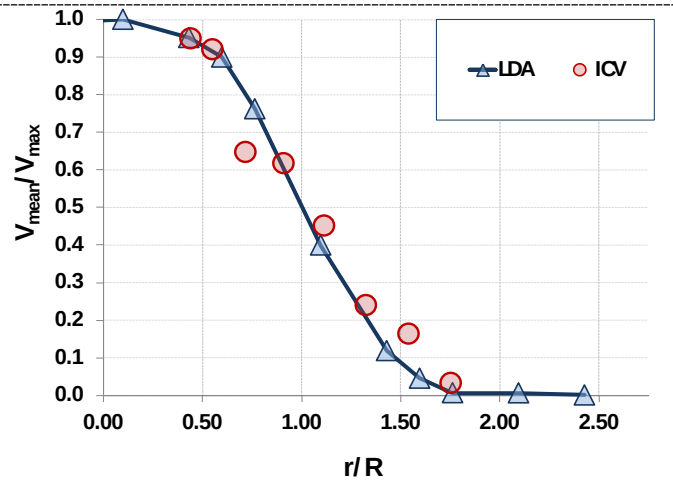

Figure 10. Radial profiles of mean velocity at x/D = 2; 4 in pipe jet; 660 GPM. Reynolds number ~500,000.

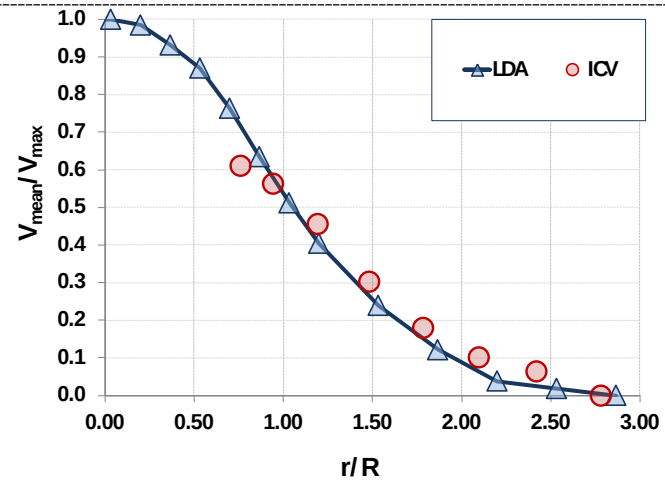

Figure 11. Radial profiles of mean velocity at x/D = 4; 4 in pipe jet; 660 GPM. Reynolds number ~500,000.

Camera Selection and Operation

For operation in an ROV, the quality of camera images may be limited by the data transfer link. The camera resolution and frame rate should be set as high as memory capacity and data transfer rates allow. Frame exposure time should be as short as necessary to freeze the motion of the fastest visible features.

When memory or data transfer capabilities limit the frame rate, suitable frame rates can be estimated using turbulence theory. This is discussed below.

Turbulent eddies, such as those visible at the boundary of a submerged oil jet, have and range of sizes and lifetimes. The lifetime of a turbulent eddy is proportional to its size, with smaller eddies having shorter lifetimes. The key parameter in describing the sizes and persistence of turbulent eddies is the turbulent dissipation rate, ε, [Hinze] which is on the order of

$$\varepsilon \sim u^3/l \sim (4/\pi)^3 (Q^3/D^7)$$

where u and l are the velocity and length scales of the largest eddies, Q is the discharge rate, and D is the jet diameter. Energy from turbulent eddies is dissipated through viscous interaction by the smallest eddies. The size of the smallest eddies, called the viscous scales or Kolmogorov scales, is represented by η, where

$$\eta = 1 / k_d \sim (\nu^3 / \varepsilon)^{1/4}$$

where ν is the kinematic viscosity and k_d the wavenumber. The size of the largest eddies is on the order of the jet diameter. The ratio of the Kolmogorov scales to the size of the largest eddies is

$$\eta / l = Re^{3/4}$$

where Re is the Reynolds number

$$Re = UD/\nu \sim Q/\nu D.$$

In the intermediate range of eddy sizes, (l, η), also called the universal equilibrium range or the inertial subrange, the eddies of a given wave number have eddy lifetimes of t_k and eddy turnover velocity u_k scales that are independent of viscosity,

$$t_k \sim (\varepsilon k^2)^{-1/3} \sim u^{-1}(k^2/l)^{-1/3}$$

$$u_k \sim (\varepsilon /k)^{1/3}$$

The camera framing rate should be sufficiently high so that the eddy does not *rotate* significantly between successive frames, i.e.,

$$f >> (\varepsilon k^2)^{1/3}$$

where k is the desired eddy wavenumber for tracking visible features. For automated analysis, the marker wavenumber, k, is selected based on the interrogation window size, $w \times w$, in units of pixels, and $1/k$ should be much smaller than the window size

$$k >> 1/w$$

Finally, we have

$$f >> >> (\varepsilon/w^2)^{1/3}$$

n lieu of the double >> signs, we suggest a factor of 10

$$f \sim 10\,(\varepsilon/w^2)^{1/3}$$

Using the ostensible parameters, an equation is derived for estimating required camera frame rates

$$f \sim 10(Q/D^{7/3})\, w^{-2/3}$$

Using the DWH post riser-cut jet as an example, let's assume a pixel covers an area of 10^{-3} x 10^{-3} m (1000x1000 pixels camera looking at a 1m x 1m area), so $w = 10^{-3}$ m, $Q = 0.1$ m^3/s (53,000 bbl/day), $D = 0.5$ m, and an interrogation area of 32 x 32 pixels is used. A suitable frame rate is estimated to be

$$f \sim 10(Q/D^{7/3})w^{-2/3} \sim 50 \text{ frames/sec}$$

For dyed jet water tank experiments done at UC Berkeley for this project, a typical pixel size was 10^{-4} m (1000x1000 pixels camera looking at a 0.1m x 0.1m area), Q=1x10^{-4} m^3/s, D=0.013 m, and w=64 pixel. So the required frame rate is estimated to be

$$f \sim 10\,(Q/D^{7/3})w^{-2/3} \sim 1000 \text{ Hz}$$

UC Berkeley PIXTif Software

UC Berkeley has developed and tested a field deployable video analysis software package which is able to provide in the field sufficiently accurate flow rate estimates for initial responders in accidental oil discharges in submarine operations. The tool is called "UCB Plume." The essence of the approach is based on tracking coherent features at the interface in the near field of immiscible turbulent jets.

The software package is ready to be used by the first responders for field implementation. We have tested the tool on submerged water and oil jets which are made visible using fluorescent dyes. We have been able to estimate the discharge rate within 20% accuracy.

A high end WINDOWS laptop computer is suggested as the operating platform and a USB connected high speed, high resolution monochrome camera as the imaging device are sufficient for acquiring flow images under continuous unidirectional illumination and running the software in the field. Results are obtained over a matter of minutes.

References

Abdel-Rahman, A. A., Chakroun, W., and Al-Fahed, S. F., 1997. "LDA measurements in the turbulent round jet," *Mechanics Research Communications*, **24**:277-288.

FRTG Plume Analysis Team, 2010, "Deepwater Horizon Release Estimate of Rate by PIV," www.doi.gov/deepwaterhorizon

Gore, J. P., and Jian, C. Q., 1993. "Analytical solution to the flame trajectory based on the analysis of "Scaling of buoyant turbulent jet diffusion flames" by N. Peters and J. Gottgens," *Combust. Flame*, **93**:336-337.

Hill, B. J., 1972. "Measurement of local entrainment rate in the initial region of axisymmetric turbulent air jets," *J. Fluid Mech.*, 51:773-779.

Hinze, O.J., "Turbulence," 1975.

Kim, J. S., Yang, W, Kim, Y., and Won, S. H., 2009. "Behavior of buoyancy and momentum controlled hydrogen jets and flames emitted into the quiescent atmosphere," *Journal of Loss Prevention in the Process Industries*, **22**:943-949.

Meijering, E., et al., "Methods for Cell and Particle Tracking," Methods in Enzymology, vol. 504, February 2012, pp. 183-200

Meijering, E. et al., "MTrackJ: A motion analysis and tracking plugin for ImageJ," http://www.imagescience.org/meijering/software/mtrackj/

McNutt, M. K., Camilli, R., Crone, T. J., Guthrie, G. D., Hsieh, P. A., Ryerson, T. B., Savaş, Ö.& Shaffer, F., 2011, Review of flow rate estimates of the Deepwater Horizon oil spill. *PNAS: Proceedings of the National Academy of Sciences of the United States of America.* Published online on December 20, 2011. DOI: 10.1073/pnas.111213910

Mi, J., Kalt, P., Nathan, G. J., and Wong, C. Y., 2007. "PIV measurements of a turbulent jet issuing from round sharp-edged plate," *Exp. Fluids*, **42**:625-637.

Mi, J., Nathan, G. J., and Nobes, D. S., 2001. "Mixing characteristics of axisymmetric free jets from a contoured nozzle, and orifice plate and a pipe," *J. Fluids Eng.*, **123**:878-883.

Nathan, G. J., Mi., J., Alwahabi, Z. T., Newbold, G. J. R., and Nobes, D. S., 2006. "Impacts of a jet's exit flow pattern on mixing and combustion performance," *Prog. Energy Combust. Sci.*, **32**:496-538.

Peters, N., and Gottgens, J., 1991. "Scaling of buoyant turbulent jet diffusion flames," *Combust. Flame*, **85**:206-214.

Quinn, W. R., 2006. "Upstream nozzle shaping effects on near field flow in round turbulent free jets," *European Journal of Mechanics B/Fluids*, **25**:279-301.

Richards, C. D., and Pitts, W. M., 1993. "Global density effects on the self-preservation behavior of turbulent free jets," *J. Fluid Mech.*, **254**:417-435.

Ricou, F. P., and Spalding, D. B., 1961. "Measurements of entrainment by axisymmetrical turbulent jets," *J. Fluid Mech.*, 11:21-32.

Schneider, C.A., Rasband, W.S., Eliceiri, K.W. "NIH Image to ImageJ: 25 years of image analysis," Nature Methods 9, 671-675, 2012.

Shaffer, F. Savas, Ö., Lee, K., de Vega, G., "Determining the Discharge Rate from a Submerged Oil Leak Jet using ROV Video," Flow Measurement & Instrumentation, v. 43, 2015.

Tseng, Q. et al., 2000, Spatial Organization of the Extracellular Matrix Regulates Cell–cell Junction Positioning. PNAS (2012).doi:10.1073/pnas.1106377109

Tseng, Qingzong. 2011. “Study of multicellular architecture with controlled microenvironment”. Ph.D. dissertation, Université de Grenoble. http://tel.archives-ouvertes.fr/tel-00622264.

Tseng, Q., 2013, “Template Matching and Slice Alignment--- ImageJ Plugins,”https://sites.google.com/site/qingzongtseng/piv